

Effect of Cathode Position on Hall-Effect Thruster Performance and Cathode Coupling Voltage

Jason D. Sommerville* and Lyon B. King†

Michigan Technological University, Houghton, Michigan 49931, USA

Hall-effect thruster performance as a function of cathode position is explored through a series of experiments in which performance is monitored while the cathode is translated via a 2-axis motion table. Significant changes in thrust, efficiency, and cathode coupling voltage are observed. Efficiency changes as great as 12% are measured. Cathode coupling voltages typically move closer to ground as the cathode is moved away from the thruster in the radial direction and as it is moved forward of the exit plane. Corresponding improvements in performance are measured. However, the improvements in performance are greater than can be explained by the change in cathode coupling voltage alone.

Nomenclature

a	Acceleration losses
e	Electronic charge
f_i	Propellant ionization fraction
I	Anode supply current
m_i	Mass of a xenon ion
n_q	Density of xenon neutral or ion with charge state q
$\langle q \rangle$	Average xenon species charge number
T	Thrust
t	Time
T_f	Final measurement of thrust with thruster off. (Thrust stand drift.)
$\langle v \rangle$	Magnitude of the average exit velocity of the HET beam
V	Discharge voltage. Potential difference between the anode and the cathode.
V_{acc}	Maximum ion beam acceleration potential
V_{cg}	Cathode coupling voltage (< 0)

Symbols

η	Thruster efficiency
η_{cg}	Efficiency due to cathode coupling
η_{other}	Other HET efficiency terms

I. Introduction

Hall-effect thrusters (HETs) are a class of electric propulsion devices that use electric and magnetic fields to create a plasma and expel the ions at high velocity in order to generate thrust.¹ A critical component of the HET is the cathode. The cathode in an HET is a plasma source which provides free electrons which serve two purposes. The first purpose is beam neutralization—sufficient electrons are expelled via the cathode to balance the charge emitted by the ion beam. The second purpose is to provide the “seed” electrons which initialize and sustain the plasma discharge near the exit plane of the HET.

The cathode coupling voltage (V_{cg}) is one of the most important parameters in the cathode coupling problem. In the laboratory, this parameter is the potential difference between the cathode and ground, i.e. the tank walls, and is

*ME-EM Dept., 815 R.L. Smith Bldg., 1400 Townsend Dr., AIAA Student Member

†AIAA Member

always a negative value. In space, the concept remains valid, the ground of the tank walls being replaced with the plasma potential infinitely far from the spacecraft. Since the anode is usually referenced to the cathode, the maximum potential through which the beam ions fall is $V_{acc} = V + V_{cg}$ and the maximum energy that can be imparted to an beam ion is qeV_{acc} . To illustrate this, Figure 1 schematically compares a low coupling volage, V_{cg1} , to a high coupling voltage, V_{cg2} . Note that in both cases the anode voltage, V , is the same. Therefore, lower (further from ground) coupling voltages give rise to greater losses in the thruster efficiency.

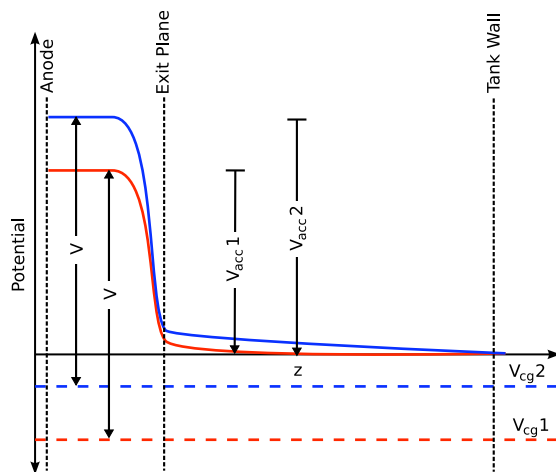


Figure 1: The available acceleration voltages, V_{acc} , for low and high cathode coupling voltages, V_{cg1} , and V_{cg2} .

The coupling voltage provides a measure of how easily electrons are transported from the cathode to the anode. Visualizing the electric circuit between the cathode and the anode as a simple ohmic circuit, lower voltages (that is, greater in magnitude) imply that there is a larger resistance between the cathode and the anode, and therefore more energy is lost in the process of providing electrons to the discharge chamber of the cathode.

The process by which the free electrons in the plume of the cathode are coupled to the anode of an HET and how this process affects cathode coupling voltage and thruster performance is not well understood. A few researchers have studied the effects of cathode type² and mass flow rate^{2,3} on HET performance. Albaréde, et al. compared three types of thermionic orificed cathodes and found only small differences in behavior.² Both Albaréde, et al. and Tilley, et al. observed increases in cathode coupling voltage with increasing flow rate, and Albaréde, et al. also noticed non-monotonic changes in anode current fluctuation frequency with changes in cathode mass flow.² It has been repeatedly noted that cathode placement has an effect on thruster performance.⁴⁻⁶ Hofer, et al. noticed significant performance improvements by placing the cathode in the center of the HET rather than outside,⁴ and Beal, Galimore and Hargus have inferred from probe measurements that cathode placement and number in an HET cluster will affect performance.⁶ However, to the best of our knowledge, only the study by Tilley, et al. specifically addresses the effect of cathode position on HET performance and is available in the literature.³ In that study, the authors note an increase in cathode coupling voltage as the cathode is moved forward of the exit plane.

There has been recent interest in the field of electric propulsion in scaling thrusters to lower voltages in order to achieve high thrust-to-power ratios.⁷⁻¹⁰ As V is decreased, the same coupling voltage represents a greater efficiency hit as it becomes a larger portion of the total available voltage. Therefore any optimization in the cathode coupling voltage at low thruster voltage may represent a significant gain in thruster efficiency.

II. Experiment

As a first step in gaining a greater understanding of cathode to HET coupling, we have undertaken a series of experiments studying the performance of an HET as a function of radial and axial cathode position. Given the interest in low power HETs, we have operated at voltages from 300 down to 150 V at optimal magnet current. For select operating voltages we have also varied the magnet current to sub- and super-optimal values. All experiments were performed with a BPT-2000 HET and a laboratory cathode at Michigan Tech's Ion Space Propulsion Laboratory.

A. Equipment

1. Vacuum Facility

All experiments were run in the Xenon Vacuum Facility at Michigan Tech's Ion Space Propulsion Laboratory. The facility is a 4-m-long chamber 2 m in diameter. It is evacuated by two 48-inch cryogenic pumps capable of 60,000 L/s each. The base pressure during these experiments was 1.3×10^{-5} Torr and operating pressures were 3.8×10^{-5} Torr as measured by an ion gauge corrected for xenon and located in the back third of the chamber.

2. Hall Thruster

The HET used in this experiment was an Aerojet BPT-2000, 2 kW class thruster.¹¹ The thruster has an outer diameter of ~100 mm and a channel width of ~10 mm. It operates at a nominal voltage of 300 V and a mass flow of 5 mg/s xenon. At these conditions its specific impulse is ~1700 s with ~50% efficiency.

3. Cathode

The cathode used in these experiments was a laboratory cathode similar to the MIREA cathode used by Albadère.² It is shown schematically in Figure 2. The cathode consists of a 1-inch-diameter titanium cylinder approximately 100 mm long. A 2-mm orifice was drilled in one face. Pressed against this hole is a molybdenum pellet holder which holds a lanthanum-hexaboride (LaB₆) emitter. Xenon is introduced into the cathode via a feed tube attached to the side of the cylinder. Filling the length of the cathode from the pellet holder to the base is a tungsten heater coil which heats the emitter to its operating temperature. Radiation insulation loosely wraps the heater and pellet holder to maximize emitter heating. A keeper electrode is positioned approximately 3 mm outside of the orifice and is used to ignite and maintain the cathode discharge.

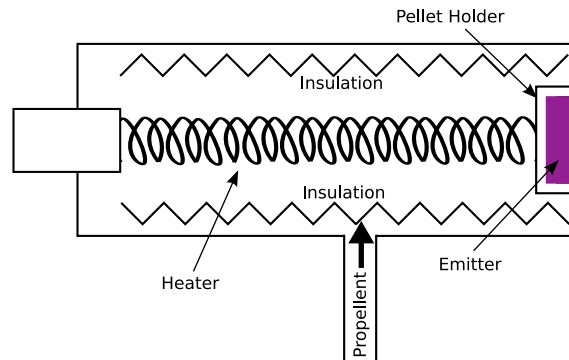


Figure 2: Schematic representation of the laboratory cathode

4. Mass Flow Controllers

Flow of xenon to the thruster and the cathode was controlled by MKS Type 1479a mass flow controllers. Their accuracy has been tested by monitoring the rise in pressure of a small calibration tank of known volume while flowing gas into the tank. The mass flow controllers are accurate to 5% of the full scale reading: 200 SCCM (19.5 mg/s xenon) for the anode controller, and 20 SCCM (1.95 mg/s xenon) for the cathode controller.

5. Thrust Stand

The thrust stand is a NASA-Glenn style, null displacement, inverted pendulum thrust stand, with automatic leveling. The displacement nulling is provided by a solenoid driven by a closed-loop digital controller which reads the displacement on an LVDT. The level is read by an electrolytic inclinometer, and controlled by a microstepping motor connected to an 80-threads-per-inch screw. The thrust is directly proportional to the current provided to the solenoid. Calibration is provided by a linear fit to a set of known weights applied to the thruster across a pulley and controlled via a stepper motor.

The closed loop controls on this thrust stand were recently implemented, and these experiments were the first to take advantage of them. During the experiment, it became clear that the level control was less than optimal. The stepper motor introduced excessive vibrations into the system which were recorded as vibrations in the thrust. Additionally, the screw attached to the stepper motor did not always rotate the same distance as the stepper motor. Rather, the screw would torque, and then eventually release several updates worth of rotation in a single, jarring motion. Averaging the thrust over a minute or two served to partially mitigate these problems.

Despite the continuous leveling, we recorded drifts in thrust measurements over time under some operating conditions. We confirmed these drifts as measurement errors by noting the thrust measurement after thruster shutdown. If no drift occurred, the thrust stand would read approximately zero thrust. In some cases, however, the thrust stand drifted as much as 5 mN over 120 minutes. The source of the drift is not entirely clear. We believe that it is a thermal drift causing changes in level perpendicular to the thruster axis to which the thrust stand controller is blind. However, it is possible for changes in the perpendicular level to couple to the parallel displacement through imbalanced material properties and imperfections in machining on the thrust stand.

To attempt to correct the drifts in thrust stand level, we have assumed a linear drift over the period from thruster turn on to thruster turn off. The slope of the drift is assumed to be T_f/t and the final thrust is given by

$$T(t) = T_{meas} - T_f/t. \quad (1)$$

The efficiency is calculated from the thrust according to

$$\eta = \frac{T^2}{2\dot{m}IV}. \quad (2)$$

Given the drifts in the thrust stand compounded with the error in the linear fit, the error in the thrust measurement is estimated at 5%. Propagating the errors of the thrust measurement and the mass flow rate through the efficiency equation, we estimate the error on the efficiency measurements at 9% of the stated efficiency values.

B. Cathode Position Experiment

To quantify the effect of cathode position on thruster performance, we ran the BPT-2000 mounted on the thrust stand, while moving the cathode through radial and axial sweeps. Data acquisition hardware and software was used to record thrust, anode current, mass flow, and cathode coupling voltage. Thruster efficiency was calculated by the software according to Equation 2.

For these tests the cathode was mounted on a two-axis motion table as shown in Figure 3. This setup enabled us to place the cathode at radial displacements of $0 \leq r \leq 250$ mm where 0 is as close to the thruster as the cathode can be positioned without contacting it (see close-up in Figure 3). At radial displacements greater than or equal to 50 mm the cathode could be positioned at axial displacements of $-295 \text{ mm} \leq z \leq 900$ mm where at $z = 0$ the cathode face is even with the thruster face.

Several radial sweeps were performed at varying thruster operating conditions. Sweeps were typically conducted from $0 \leq r \leq 200$ mm in 10 mm increments. Table 1 shows the complete list of operating conditions. All conditions were performed with cathode mass flow rates of ~ 1 mg/s.

Table 1: Cathode Position Tests

Test	V (V)	\dot{m} (mg/s)	I_{mag} (A)	Optimization	Sweep
Test 1a	300	5.0	4.20	Optimal	$0 \leq r \leq 200$ mm
Test 1b	300	5.0	3.15	Suboptimal	$0 \leq r \leq 200$ mm
Test 1c	300	5.0	5.25	Superoptimal	$0 \leq r \leq 200$ mm
Test 2a	250	4.0	2.5	Optimal	$0 \leq r \leq 200$ mm
Test 2b	250	4.0	2.1	Suboptimal	$0 \leq r \leq 200$ mm
Test 2c	250	4.0	3.15	Superoptimal	$0 \leq r \leq 200$ mm
Test 3	200	4.0	2.1	Optimal	$0 \leq r \leq 200$ mm
Test 4	150	4.0	0.6	Optimal	$0 \leq r \leq 200$ mm
Test 5	250	4.0	2.5	Optimal	$-150 \text{ mm} \leq z \leq 900$ mm

During each test the thruster was allowed to run at the operating point for at least 30 minutes prior to recording data to allow the thruster, cathode, and thrust stand to reach thermal equilibrium. After this period, the thruster was

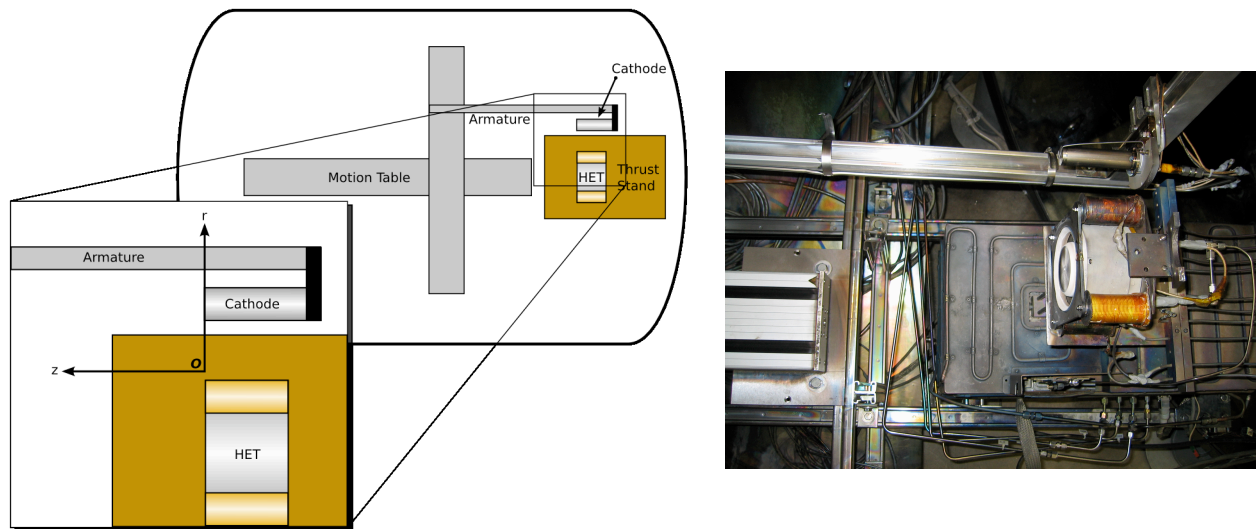


Figure 3: Experimental setup

turned off, and thrust stand calibration performed. The calibration procedure typically required three minutes. Then, the thruster was run for two to three minutes at each of the cathode positions and the thrust data averaged over this period. The positions were selected in random order to avoid correlations between any temporal changes in thruster or thrust stand performance with changes due to cathode position. After all positions were measured, the thruster was turned off and any offset from 0 thrust measured by the thrust stand recorded (see Section 5).

In all cases, the thruster was first operated at its most efficient magnetic field, as determined by adjusting the magnetic current while monitoring the efficiency calculated in real time by the thrust stand software. This optimization was performed with the cathode at the origin. We later discovered that in nearly all cases this was the least efficient cathode position, and future tests will be optimized with the cathode in a better position. For consistency, the procedure was continued throughout all of the data presented here.

In Test 1 and Test 2, the 300 V and 250 V cases, the magnet current was adjusted above and below the optimal values. For the Test 1, values 25% above and below the optimal were chosen. For the Test 2, whose optimal magnet current was 2.5 A, values of 3.15 A and 2.1 A were chosen for the super- and sub-optimal currents because they matched magnet currents used in Test 1 and Test 3 respectively. Future tests are planned which will extend the procedure of magnet current adjustment to all cases.

III. Results

Figures 4 and 5 plot thrust, efficiency, anode current, and cathode coupling voltage as a function of cathode radial position for each of the radial tests. In all cases, when the cathode was near the thruster, particularly at $r = 0$, significant heat was exchanged between the cathode and the anode. This was evidenced by an increase in voltage in the current-limited supplies for the cathode heater and the magnet coils. This heat exchange made it difficult to achieve thermal equilibrium and the error on these data points is therefore significantly higher than on those where the cathode is positioned further from the thruster.

Test 1 is at the nominal operating point for the thruster. For all magnet currents, the cathode coupling voltage trends upwards as the cathode is moved away from the thruster, changing by approximately 10 V, or 3% of the discharge voltage. The anode current holds steady and the thrust increases, resulting in an efficiency increase of approximately 3% to 5%.

During Test 1c it was necessary to restart the thruster. The numbered points in Figure 4(c) show the order in which the points were taken, and the asterisk denotes the first point after the restart. We noted that the cathode coupling voltages did not return to exactly the same position after the restart.

Test 2, run at a discharge voltage of 250 V, shows the most interesting behavior. All magnetic field conditions exhibited a peak in cathode coupling voltage between 40 and 60 mm, followed by a trough between 80 and 100 mm, and then a gradual rise as the cathode was moved out to 200 mm. Again the discharge current held constant, while the thrust and efficiency tracked the changes in cathode coupling voltage.

Test 3, run at a discharge voltage of 200 V, also exhibits anomalies due to thruster restarts. Again, the plot shows the order in which the data were taken, with asterisks denoting the first point after a thruster restart. Note that there is a significant jump in cathode coupling voltage after the restart between points five and six. In particular, the cathode coupling voltage dropped by approximately 2 V between points thirteen and five. We believe that some of this drop is attributed to the change in conditions between thruster restarts. However, the magnitude of the change in cathode coupling voltages across the range of cathode positions is much smaller than in either Test 1 or Test 2.

Test 4, at a discharge voltage of 150 V, shows drastically different behavior than the previous tests. Here the cathode coupling voltage significantly decreases with increasing radial distance. The thrust and efficiency also decrease, somewhat in step with the cathode coupling voltage. Note also that the discharge current, in contrast to the other cases, changes drastically with cathode position.

Test 5, performed at the optimal magnet current and discharge voltage of 250 V, is the only axial sweep performed in this study. Here, the cathode was placed 50 mm away from the thruster, radially. As the cathode was moved behind the thruster poor performance is recorded, along with low cathode coupling voltages. As the cathode was brought downstream of the cathode the performance of the thruster and cathode coupling voltage improved significantly, reaching a peak at 175 mm downstream of the exit plane. The anode current is seen to vary slightly, but consistently, with the other measurements. This change in current is small in comparison to Test 4, but certainly much more pronounced than the remainder of the radial sweeps.

IV. Discussion

A. Theoretical Effect of Cathode Coupling Voltage on Performance

The cathode coupling voltage plays an important role in determining the overall performance of the thruster. As previously mentioned, cathode couple voltage provides a measure of how easily cathode electrons are transported from the cathode to the discharge chamber of the HET. Recall that the maximum voltage through which the HET ions may be accelerated is $V_{acc} = V + V_{cg}$ (where V_{cg} is negative). The thrust is given by

$$\mathbf{T} = \dot{m}\langle\mathbf{v}\rangle. \quad (3)$$

Invoking a loss term a , which incorporates cosine losses, ions which are created below the peak of the potential hill, and all other acceleration inefficiencies, the averaged exit velocity of the ions and the neutrals may be expressed as

$$\langle v \rangle = a \sqrt{\frac{2\bar{q}e(V + V_{cg})}{m_i}}. \quad (4)$$

Here \bar{q} is the average charge of all xenon species, ions and neutrals, i.e.

$$\bar{q} \equiv \frac{\sum_{q=0}^{54} qn_q}{\sum_{q=0}^{54} n_q}. \quad (5)$$

Substituting Equations 3 and 4 into Equation 2 yields

$$\eta = \frac{a^2\bar{q}e\dot{m}(V + V_{cg})}{m_iIV} \quad (6)$$

$$= a^2 \left(\frac{\bar{q}e\dot{m}}{m_iI} \right) (1 + V_{cg}/V). \quad (7)$$

$1 + V_{cg}/V$ is clearly an efficiency term, as is a^2 . The first group of terms in parentheses is the current efficiency, as defined by Ross and King.¹² Defining

$$\eta_{other} \equiv a^2 \left(\frac{\bar{q}e\dot{m}}{m_iI} \right) \quad (8)$$

$$\eta_{cg} \equiv 1 + V_{cg}/V \quad (9)$$

we see that the total efficiency of the thruster is given by

$$\eta = \eta_{other}\eta_{cg}. \quad (10)$$

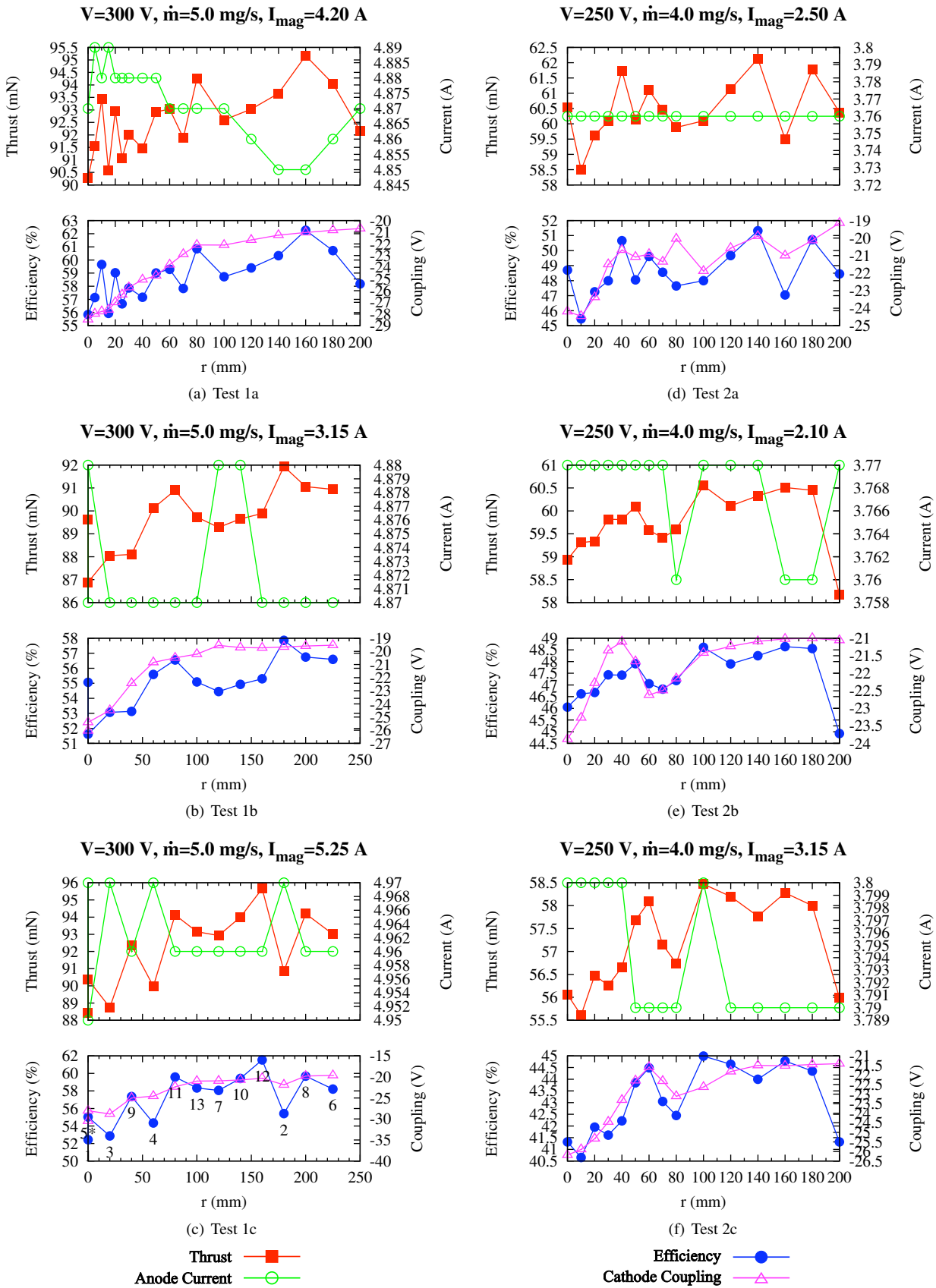


Figure 4: Results of the cathode position test

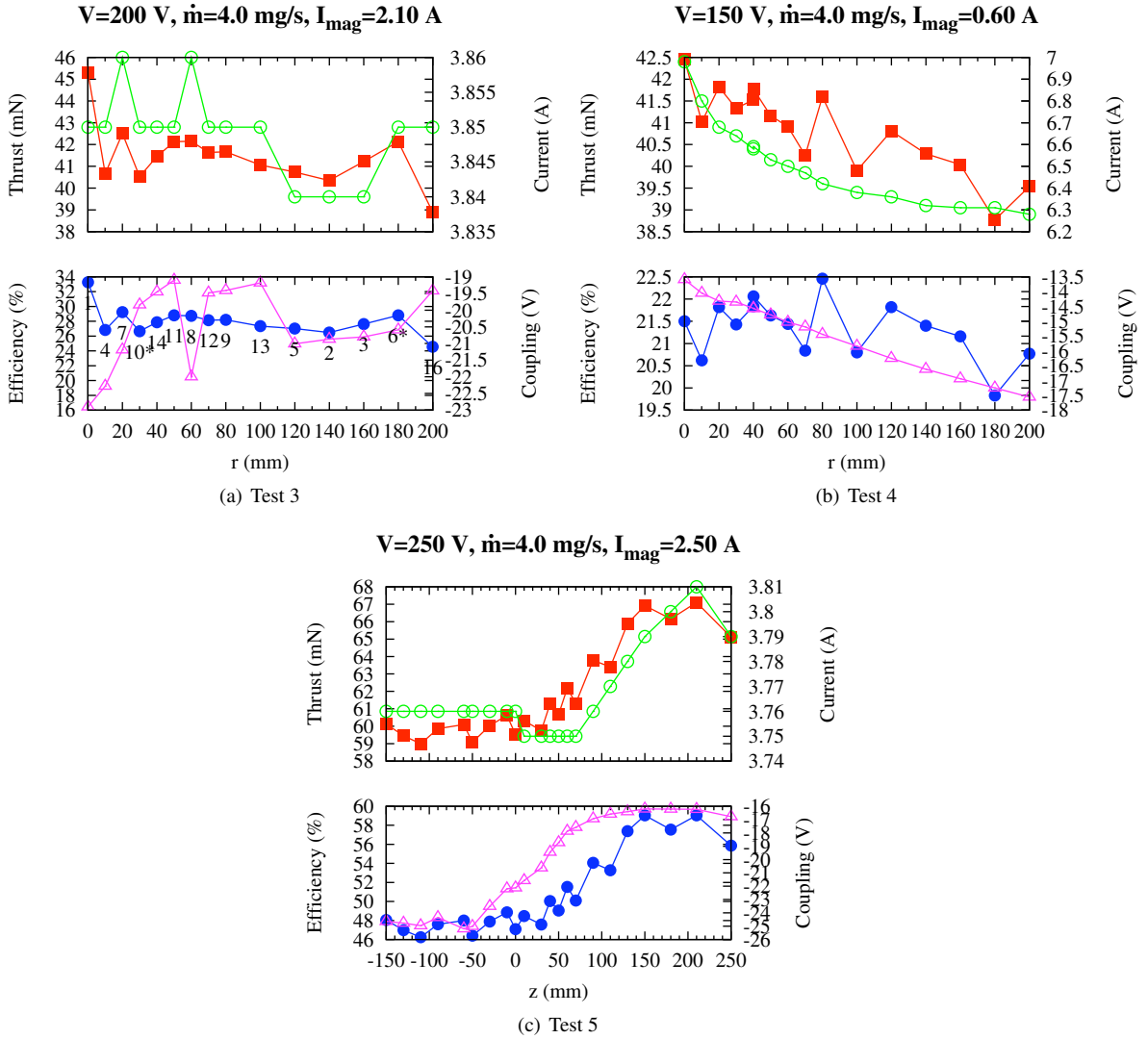


Figure 5: Results of the cathode position test (continued)

Therefore, the maximum improvement in thruster efficiency possible by raising the cathode coupling voltage is given by

$$\eta_{\max} - \eta = \eta_{\text{other}}(100\% - \eta_{cg}) \quad (11)$$

if η_{other} is independent of V_{cg} .

B. Observed Cathode Coupling Voltages

Because the cathode coupling voltage plays a significant role in determining the efficiency of the thruster, a careful look at how its behavior changes with the parameters studied is warranted. In all of the test cases presented above the cathode coupling voltage is seen to vary with cathode placement. Figure 6 shows the cathode coupling voltages for each of the anode voltages explored at optimized magnet current. One notes a general decrease in coupling voltage with increasing anode voltage. This is better seen in Figure 7. While the trend is clear, it is unclear whether the change in coupling voltage should be attributed to the change in voltage or the change in magnetic field. A most interesting feature also appears between the 200 and 150 V cases, where a drastic change in behavior is seen. We suspect that this change in behavior is not due to the change in anode voltage, but rather to the change in magnet current, and therefore magnetic field, required to operate the thruster stably at low voltage. Note that the optimal magnet current for 150 V is significantly less than the optimal current for 200 V.

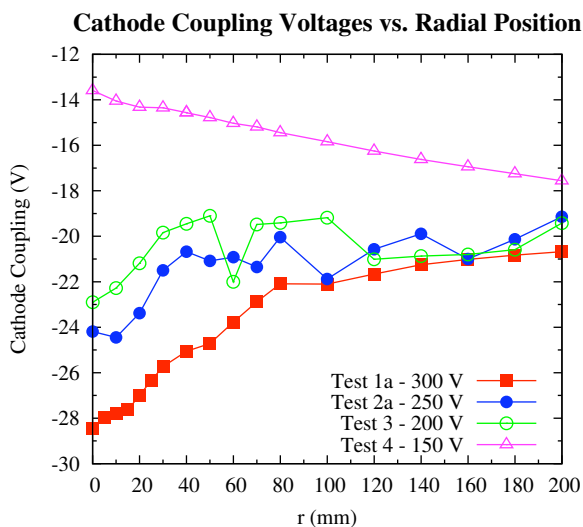


Figure 6: Cathode coupling voltages for all radial sweep tests at optimal magnet currents. The number in the legend indicates the anode voltage.

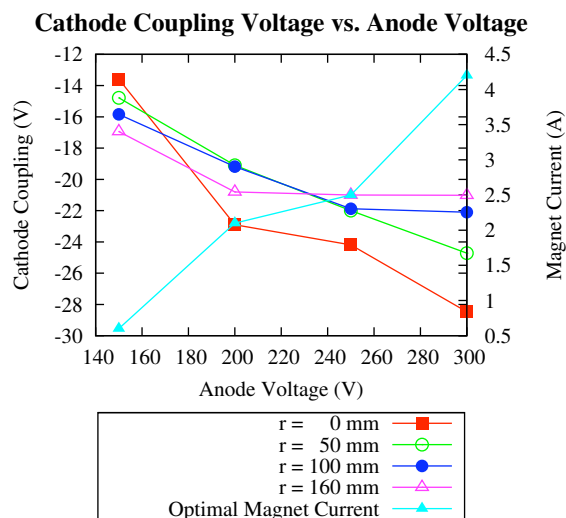


Figure 7: Cathode coupling voltages at optimal magnet current for select radial positions as a function of anode voltage.

In an attempt to better understand the effect of magnetic field strength decoupled from anode voltage, Figure 8 shows the coupling voltage for select cathode displacements as a function of magnet current. For the same anode voltage, increasing magnetic field strength generally corresponds to decreasing (more negative) coupling voltage, though this effect weakens as the cathode is moved further away from the thruster. Ross and King have also observed this behavior while operating between 100 V and 200 V on the same thruster with fixed cathode position.¹² Phenomenologically, this is reasonable as the electrons need to cross magnetic field lines in order to enter the discharge region, and electron mobility is generally inversely proportional to magnetic field strength.

One final point of interest discovered in these data is the relatively consistent local maxima of cathode coupling found in all of the Test 2 sub-cases. All of the magnet current settings in Figure 9 show a peak somewhere between 40 mm and 60 mm followed by a trough near 80 mm. This suggests that there is a narrow optimal cathode placement for a given anode voltage, at least in some circumstances. More data are needed to understand this effect.

C. Observed Thruster Efficiency

As seen in Figures 4 and 5, thruster efficiencies in this experiment are between 20% and 50%. Typical cathode coupling voltages seen in this experiment are approximately 10% of the discharge voltage, resulting in $\eta_{cg} \approx 90\%$.

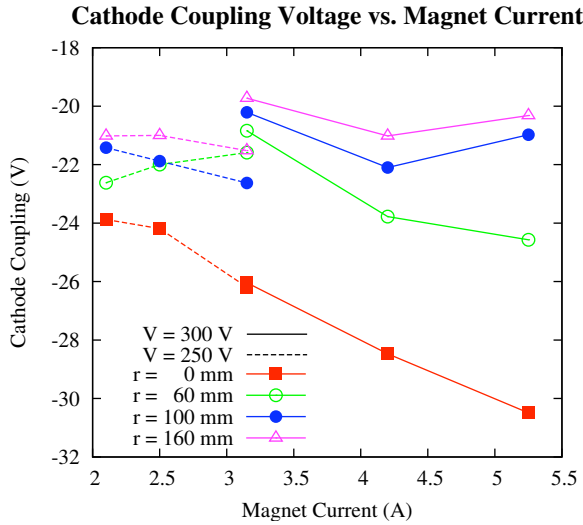


Figure 8: Cathode coupling voltages versus magnet current for the two operating voltages at which sub- and super-optimal magnet currents were set.

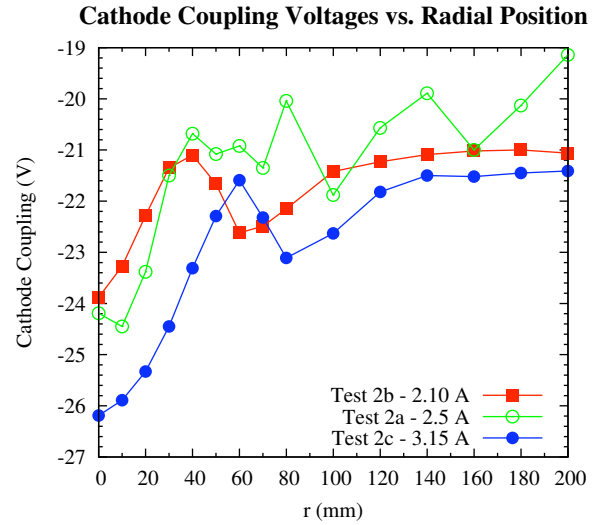


Figure 9: Cathode coupling voltages for Test 2. Note the peak near 50 mm.

Solving Equation 10 for η_{other} , this suggests the other efficiencies combined are between 22% and 56%. Substituting these values into Equation 11 we conclude that raising the cathode coupling voltage to ground will result in a maximum 2.2% to 5.6% increase in efficiency, again, assuming that η_{other} is independent of V_{cg} . Inspection of Figures 4 and 5 suggests that the changes in efficiency with cathode position are not fully accounted for by changes in cathode coupling voltage. For instance, Test 1b, in Figure 4(b), shows a 7% increase in efficiency for a 3% change in cathode coupling voltage with respect to the discharge voltage. The 3% change in cathode coupling voltage only accounts for about 1.7% of the total 7% improvement. This suggests that either η_{other} is not independent of V_{cg} , that cathode position affects both V_{cg} and η_{other} independently, or both.

The axial position sweep in Test 5 provides the clearest evidence for the connection between thruster performance, cathode coupling voltage, and cathode position. It is unclear why the axial sweep provided a larger change than the radial sweeps. Obviously, the cathode was placed in a region where the electrons are more easily conducted to the anode. Possible explanations are that this is due to changes in magnetic field, due to the obvious change in plasma conditions (having moved into the plume), or some combination of the two.

V. Conclusions and Future Work

The means by which the cathode electrons are conducted to the discharge chamber, and their affect on cathode coupling voltage are not well understood. A better understanding of this behavior would give thruster system designers a set of tools for optimizing thruster performance without resorting to time consuming and expensive testing. The data presented here are necessary to test developing HET-cathode coupling theory.

These data clearly show that cathode coupling voltage and thruster performance are affected by radial and axial position and by magnetic field strength. Furthermore, the changes in cathode coupling voltage are insufficient to completely explain the changes in thruster performance through the effect of cathode coupling on acceleration potential. Therefore, either cathode position directly effects thruster efficiency, or cathode coupling voltage effects thruster behavior in a more complicated fashion than has been presented here.

We are planning future tests that will further explore the performance of the thruster with axial position. While this will provide additional data against which to test cathode coupling theories, a better understanding of the magnetic and plasma conditions in this region is also required. Therefore, we are also planning to investigate the effect of the magnetic field on the coupling through magnetic field modeling combined with electrostatic probe studies of the region between the cathode and the thruster.

Acknowledgments

The authors give their thanks to Mr. Jerry Ross of Michigan Tech and Dr. Bill Larson of the Air Force Research Laboratory for their discussions of thruster efficiency, to Aerojet for the donation of the BPT-2000 used in this research, and to Mr. Marty Toth for the fabrication of the cathode. This research is funded by the Air Force Office of Scientific Research and the National Science Foundation.

References

- ¹R. G. Jahn, *Physics of Electric Propulsion*. McGraw-Hill Series in Missile and Space Technology, New York: McGraw-Hill Book Company, 1968.
- ²L. Albarède, V. Lago, P. Lasgorceix, M. Dudeck, A. Burgova, and K. Malik, "Interaction of a hollow cathode stream with a Hall thruster," in *28th International Electric Propulsion Conference*, vol. IEPC-03-333, Electric Rocket Propulsion Society, March 17–21 2003.
- ³D. L. Tilley, K. H. de Grys, and R. M. Myers, "Hall thruster-cathode coupling," in *35th AIAA/ASME/SAE/ASEE Joint Propulsion Conference*, vol. AIAA-99-2865, June 20–24 1999.
- ⁴R. R. Hofer and A. D. Gallimore, "Recent results from internal and very-near-field plasma diagnostics of a high specific impulse Hall thruster," in *28th International Electric Propulsion Conference*, vol. IEPC-2003-037, March 17–21 2003.
- ⁵R. R. Hofer, L. K. Johnson, D. M. Goebel, and D. J. Fitzgerald, "Effects of an internally-mounted cathode on hall thruster plume properties," in *42st AIAA/ASME/SAE/ASEE Joint Propulsion Conference*, vol. AIAA-2006-4482, July 9–12 2006.
- ⁶B. E. Beal, A. D. Gallimore, and W. A. Hargus, "The effects of cathode configuration on hall thruster cluster plume properties," in *41st AIAA/ASME/SAE/ASEE Joint Propulsion Conference*, vol. AIAA-2005-3678, July 10–13 2005.
- ⁷M. Patterson, S. P. Grisnik, and G. C. Soulas, "Scaling of ion thrusters to low power," in *25th International Electric Propulsion Conference*, vol. IEPC 97-098, August 24–28 1997.
- ⁸D. H. Manzella and D. Jacobson, "Investigation of low-voltage/high-thrust Hall thruster operation," in *39th AIAA/ASME/SAE/ASEE Joint Propulsion Conference*, vol. AIAA-2003-5004, July 20–23 2003.
- ⁹A. A. Smirnov, Y. Raitses, and N. J. Fisch, "Parametric investigation of miniaturized cylindrical and annular Hall thrusters," *Journal of Applied Physics*, vol. 92, pp. 5673–5679, November 2002.
- ¹⁰J. Ashkenazy, J. Shitrit, and G. Appelbaum, "Hall thruster modifications for reduced power operation," in *29th International Electric Propulsion Conference*, vol. IEPC-2005-080, October 31–November 4 2005.
- ¹¹D. King, D. L. Tilley, R. Aadland, K. Nottingham, R. Smith, C. Roberts, V. Hraby, B. Pote, and J. Monheiser, "Development of the BPT family of U.S.-designed Hall current thrusters for commercial LEO and GEO applications," in *34th AIAA/ASME/SAE/ASEE Joint Propulsion Conference*, vol. AIAA-98-3338, July 13–15 1998.
- ¹²J. L. Ross and L. B. King, "Energy efficiency in low voltage Hall thrusters," in *43rd AIAA/ASME/SAE/ASEE Joint Propulsion Conference*, vol. AIAA-2007-5179, July 8–11 2007.